Evidence for a Novel, Strongly Bound Acto−S1 Complex Carrying ADP and Phosphate Stabilized in the G680V Mutant of *Dictyostelium* Myosin II†

Taro Q. P. Uyeda,*,‡ Kiyotaka Tokuraku,‡ Kuniyoshi Kaseda,‡ Martin R. Webb,§ and Bruce Patterson||

Gene Discovery Research Center, National Institute of Advanced Industrial Science and Technology (AIST), Tsukuba, Ibaraki 305-8562, Japan, National Institute for Medical Research, Mill Hill, London NW7 1AA, U.K., and Department of Molecular and Cellular Biology, University of Arizona, Tucson, Arizona 85721

Received May 22, 2002

ABSTRACT: Gly 680 of *Dictyostelium* myosin II sits at a critical position within the reactive thiol helices. We have previously shown that G680V mutant subfragment 1 largely remains in strongly actin-bound states in the presence of ATP. We speculated that acto−G680V subfragment 1 complexes accumulate in the A·M·ADP·P_i state on the basis of the biochemical phenotypes conferred by mutations which suppress the G680V mutation in vivo [Wu, Y., et al. (1999) *Genetics 153*, 107−116]. Here, we report further characterization of the interaction between actin and G680V subfragment 1. Light scattering data demonstrate that the majority of G680V subfragment 1 is bound to actin in the presence of ATP. These acto−G680V subfragment 1 complexes in the presence of ATP do not efficiently quench the fluorescence of pyrene−actin, unlike those in rigor complexes or in the presence of ADP alone. Kinetic analyses demonstrated that phosphate release, but not ATP hydrolysis or ADP release, is very slow and rate limiting in the acto−G680V subfragment 1 ATPase cycle. Single turnover kinetic analysis demonstrates that, during ATP hydrolysis by the acto−G680V subfragment 1 complex, quenching of pyrene fluorescence significantly lags the increase of light scattering. This is unlike the situation with wild-type subfragment 1, where the two signals have similar rate constants. These data support the hypothesis that the main intermediate during ATP hydrolysis by acto−G680V subfragment 1 is an acto−subfragment 1 complex carrying ADP and P_i, which scatters light but does not quench the pyrene fluorescence and so has a different conformation from the rigor complex.

The cyclic interaction of myosin heads with actin filaments depends on ATP hydrolysis to produce force and displacement. The myosin head or subfragment 1 (S1)[1] consists of a globular domain, which contains an actin binding site and a catalytic site, and a distal, elongated light chain domain. It is widely postulated that the light chain domain acts as part of a lever arm whose swinging motion produces force and displacement. This swinging lever arm model is supported by observations using mutant myosins that the sliding velocity in vitro (*1*, *2*), and more directly, the stroke size (*3*, *4*), is proportional to the length of the lever arm. The swinging lever arm model is also supported by several structural observations (*5*−*9*), which demonstrate that the motor domain of myosin can adopt two distinct conformations with different lever arm angles relative to the actin binding site.

Scheme 1

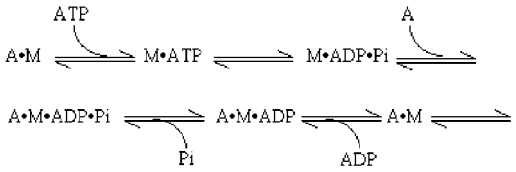

The structural information is mainly obtained using myosin heads either in crystals or free in solution, and there is little relevant information on the structure of myosin heads bound to actin filaments. It is well established that myosin heads in the absence of nucleotides bind to actin filaments at a 45° tilt angle (*10*), forming the arrowhead structure. Because addition of ATP rapidly dissociates these rigor complexes, it is generally assumed that the rigor complex is the "poststroke" conformation. What, then, is the starting conformation of the stroke, or the "prestroke" conformation?

Cyclic interaction between actin filaments and the motor domain of myosin can be summarized as shown in Scheme 1. Kinetic analysis suggested that the force production is associated with P_i release, which precedes ADP release (*11*−*13*). A major hindrance to observe the elusive prestroke acto−myosin complex is that its lifetime is extremely short, since P_i is quickly released upon formation of the A·M·ADP·P_i complex (*14*, *15*). Attempts to enrich prestroke cross-bridges, and thereby to obtain high-resolution structural information on these cross-bridges, have not been successful (*16*, *17*).

† Supported in part by a grant-in-aid from the Ministry of Science, Culture, and Education of Japan to T.Q.P.U., by an NIH grant to B.P., and by the U.K. Medical Research Council to M.R.W.

* Corresponding author. Phone: +81-298-61-2555. Fax: +81-298-61-3049. E-mail: t-uyeda@aist.go.jp.

‡ National Institute of Advanced Industrial Science and Technology.

§ National Institute for Medical Research.

|| University of Arizona.

[1] Abbreviations: DTT, dithiothreitol; EDTA, ethylenediaminetetraacetic acid; HEPES, 4-(2-hydroxyethyl)-1-piperazineethanesulfonic acid; mant-ADP, 2′(3′)-*O*-(*N*-methylanthraniloyl)-ADP; MDCC, *N*-[2-(1-maleimidyl)ethyl]-7-(diethylamino)coumarin-3-carboxamide; PBP, phosphate binding protein; S1, subfragment 1.

10.1021/bi026177i CCC: $22.00
Published on Web 06/27/2002

Thus, there is only inference derived from docking of crystal structures of the motor domain, obtained in the presence of a variety of nucleoside phosphate analogues, to the electron micrographs of the rigor acto−S1 complex regarding the structure of the prestroke conformation of the actomyosin complexes (*18*).

The failure to identify a distinct prestroke cross-bridge conformation could be explained by one of the following three hypotheses. First, the hypothetical, distinct prestroke cross-bridge state may be simply so short-lived that it eluded past investigation. If this is the case, we need to identify an experimental condition or mutation that stabilizes the prestroke conformation. Second, it may be that the "disordered" cross-bridges, which are observed in the presence of ATP, change their conformation directly to the rigor structure within each mechanical cycle. Such a disorder-to-order conformational change, when averaged, could produce force and unidirectional displacement (*19*−*21*). Third, a radically divergent model argues that actomyosin sliding is driven by stepping of the myosin head along multiple subunits of actin (*22*). This model, supported by high-resolution measurements of displacements made by single skeletal muscle S1 molecules (*23*), processive, ~36 nm stepping movement of a mutant myosin V with a short lever arm (*24*), and processive movement of single-headed class IX myosin (*25*, *26*), would make the hypothetical swinging motion of the myosin motor domain along actin filaments, either from one defined angle to another or from a random angle to a defined angle, irrelevant as a mechanism to produce force and motion. Furthermore, it may well be that there are multiple physical principles of force generation for different subclasses of myosin or even for a given type of myosin, depending on the load and speed. In any case, it is critically important to identify and characterize conformational states of the acto−S1 complex that occur immediately preceding the formation of the rigor state. A more thorough understanding of the biochemical and structural characteristics of the prestroke state is essential to distinguish between these models.

We have taken a molecular genetic approach to this challenging problem. The central goal is to isolate a mutant myosin impeded in P_i release and thereby capture and characterize the prestroke acto−myosin conformation. Our recent analyses proved that the G680V mutant myosin II of *Dictyostelium* fulfils several criteria for a stalled prestroke state (*27*). First, the G680V mutant S1 cosediments efficiently with actin filaments even in the presence of ATP, but not in the presence of ATPγS, suggesting that the mutation causes overoccupancy of an actin-bound state different from the prehydrolysis state. This is supported by the observation that, in vitro, G680V myosin moves actin filaments very slowly and strongly inhibits movement when mixed with wild-type myosin. These results suggest that the G680V myosin head spends an unusually long time bound with actin in the presence of ATP, most likely following hydrolysis. We also observed that the salt sensitivity of actin binding that the mutant exhibited in the presence of ATP differed from that in the rigor or ADP states, suggesting that the overoccupied state occurred elsewhere in the cycle. More recently, we have isolated a number of suppressor mutations for the G680V mutation on the basis of a phenotypic selection scheme (*28*). Since these alterations restore function to motors bearing the G680V defect, they must counteract its central biochemical defect. Many of these suppressor mutations, when separated from the G680V mutation, exhibit elevated MgATPase activity in the absence of actin, indicating that the rate-limiting P_i release step is accelerated in these suppressors (*29*). The fact that the defect of G680V mutation is alleviated by accelerating P_i release strongly supports our contention that its defect is at the point of P_i release. Taken together, these data support a model in which the complex of actin and the G680V mutant myosin heads accumulates in the elusive prestroke conformation carrying ADP and P_i in the presence of ATP.

To further investigate this possibility, we performed a series of biochemical analyses to characterize the complex of actin and G680V mutant myosin. These results show that the main intermediate during steady-state ATP hydrolysis of G680V S1 in the presence of actin is the acto−S1 complex carrying ADP and P_i, which is structurally distinct from the A·M·ADP or A·M state.

MATERIALS AND METHODS

Construction of Plasmids. pTIKLOE, an expression vector that carries genes for each of the two light chains and allows overexpression of S1 with bound light chains, was constructed as follows. First, the *Dictyostelium* myosin II essential light chain (ELC) gene fused with the actin 15 promoter and the N-terminally His-tagged *Dictyostelium* myosin II regulatory light chain (RLC) gene fused with the actin 15 promoter and the actin 6 terminator (both constructs carrying either of the chimeric genes were kindly provided by Dr. K. Sutoh, The University of Tokyo) were subcloned into the Litmus 28 cloning vector (New England Biolabs, Beverly, MA), such that the two genes point to each other sharing the actin 6 terminator. The resultant light chain gene cassette was inserted at the junction between the G418 resistance cassette and the *Ddp*I extrachromosomal replication sequences of pTIKL (*30*).

For the overexpression of His-tagged *Dictyostelium* S1, a polyhistidine tag sequence was fused to the RLC binding sequence, followed by the native stop codon and the terminator. The amino acid sequence at the C-terminus of this construct is LFSKAHHHHHHHHKA. An *Xba*I−*Sac*I fragment containing this His-tagged S1 gene fused with the actin 15 promoter was inserted at the *Xba*I/*Sac*I sites of pTIKLOE, yielding pTIKLS1OE. The G680V S1 gene was made by replacing a *Bst*XI−*Nco*I fragment of the wild-type S1 gene with that of pBIGMyoG680V (*27*).

Preparation of Proteins. pTIKLS1OE or pTIKLG-680VS1OE was used to transform *Dictyostelium* cells lacking the single myosin II heavy chain (*mhcA*) gene (*31*) by electroporation (*32*).

For a typical S1 preparation, 10−15 g of cells was harvested from six 30 × 30 cm^2 square dishes each containing 200 mL of medium (*33*). Wild-type S1 was purified from these cells by extraction of the cytoskeleton fraction with MgATP, followed by Ni-NTA affinity chromatography, as described previously (*33*).

It was not possible to purify G680V S1 using this protocol, due to its unusually high affinity for actin in the presence of ATP. Therefore, the following modifications were made. The washed cells were suspended in 4 volumes/g of the lysis buffer [25 mM HEPES, pH 8.0, 25 mM NaCl, 5 mM EDTA,

1 mM dithiothreitol (DTT)]. Five volumes per gram of cells of lysis buffer containing a mixture of proteinase inhibitors and 1% Triton X-100 was added, and the mixture was centrifuged at 36000*g* for 30 min. The pellets were resuspended in the wash buffer (10 mM HEPES, pH 7.4, 100 mM NaCl, 1 mM EDTA, 7 mM β-mercaptoethanol) and centrifuged at 36000*g* for 15 min. The washed pellets were extracted with 2 volumes/g of cells of the extraction buffer (10 mM HEPES, pH 7.4, 250 mM NaCl, 5 mM $MgCl_2$, 4 mM ATP, 7 mM β-mercaptoethanol) and centrifuged at 300000*g* for 15 min. G680V S1 was isolated from the supernatant by Ni-NTA affinity chromatography as above. Purified S1 fractions were dialyzed against a buffer containing 25 mM HEPES, pH 7.4, 25 mM KCl, 4 mM $MgCl_2$, and 1 mM DTT and concentrated using a Vivaspin ultrafiltration device (30000 MWCO; Vivascience, Binbrook, U.K.).

Rabbit skeletal muscle actin was prepared using the method of Spudich and Watt (*34*). Labeling of actin with pyrene was carried out according to the method of Kouyama and Mihashi (*35*).

The concentrations of actin and S1 were determined spectrophotometrically using extinction coefficients of 0.62 cm^2/mg at 290 nm for actin (*36*) and 0.80 cm^2/mg at 280 nm for S1.

Spectroscopic Measurements. Light scattering derived from the acto−S1 complex was measured as follows. A concentrated solution of S1 was added to an F-actin solution in the assay buffer (10 mM HEPES, pH 7.4, 4 mM $MgCl_2$, 25 mM KCl, 1 mM DTT) in a quartz cuvette. Final concentrations of actin and S1 were both 2 μM. This was followed by addition of 1 mM ATP. Mixing was performed manually, and changes in light scattering at 411 nm were monitored at room temperature.

Changes in fluorescence of pyrene-labeled actin were monitored in a similar way, except that excitation light of 365 nm was used and emission was monitored at 407 nm. The concentration of pyrene-labeled F-actin was 1 μM.

Stopped-Flow Measurements. Dissociation of the acto−S1 complex was monitored through changes in intensities of fluorescence of pyrene−F-actin or light scattering using a KinTek SF-2001 stopped-flow spectrophotometer equipped with a 75 W Xe lamp. Fluorescence of pyrene−actin was excited at 365 nm and detected after passing through a 389 nm cutoff filter (*37*).

Release of mant-ADP (Molecular Probes, Eugene, OR) from S1 following addition of excess ATP was monitored by excitation at 295 nm (*38*) using the 389 nm cutoff filter.

The rates of phosphate release were measured using MDCC−PBP as described previously (*39*), with some modifications. Namely, S1 at a concentration of 4 μM was incubated with 0.04 unit/mL apyrase (grade VII, Sigma), 0.02 unit/mL purine nucleoside phosphorylase, 100 μM 7-methylguanosine, 10 μM MDCC−PBP in 25 mM KCl, 4 mM $MgCl_2$, 1 mM DTT, and 10 mM HEPES, pH 7.4, for 20 min at room temperature, immediately before introduction into one of the syringes. The solution of 96 μM actin filaments was dialyzed against 25 mM KCl, 4 mM $MgCl_2$, 1 mM DTT, and 10 mM HEPES, pH 7.4, and was further treated with the Dowex anion-exchange resin (1-X8). It was then diluted 2-fold in the same buffer, supplemented with 0.02 unit/mL purine nucleoside phosphorylase, 100 μM 7-methylguanosine, and 4 μM ATP, and was transferred to the second syringe. A 460 nm interference filter was used to detect the emission light. A control experiment showed that the low concentration of apyrase present in the S1 solution does not significantly affect the results.

Transients shown are the average of three to five consecutive measurements. The temperature was 20 °C.

ATPase Assays. Steady-state ATPase activities were determined by measuring release of phosphate at 20 °C using the method of Kodama et al. (*40*). The reaction mixtures contained 25 mM imidazole (pH 7.5), 25 mM KCl, 4 mM $MgCl_2$, 1 mM DTT, and 2 mM ATP, with or without rabbit skeletal muscle F-actin.

ATP Hydrolysis Assay. [α-^{32}P]ATP was added at a final concentration of 100 μM (approximately 0.05 μCi/μL) to the rigor complex (13 μM G680V S1 and 26 μM actin filaments) in the assay buffer (10 mM HEPES, pH 7.4, 4 mM $MgCl_2$, 1 mM DTT, and 25 or 100 mM KCl) at room temperature, and the reaction was terminated by the addition of 0.2 M perchloric acid. Small aliquots of the solutions were spotted on a poly(ethylenimine)−cellulose thin-layer chromatography (TLC) plate (Merck, Darmstadt, Germany). The TLC was run in 0.7 M ammonium sulfate, and the relative amounts of ATP and ADP were quantified using a phosphorimager (Storm 830, Molecular Dynamics).

RESULTS

Overexpression of Dictyostelium S1. Studies on recombinant *Dictyostelium* S1 have been hampered by the relatively low yield of the protein. The expression levels of full-length myosin II or its fragments in wild-type or myosin II null cells are at best comparable to, and often significantly less than, that of endogenous myosin II in wild-type cells. This is despite the fact that the expression of the recombinant heavy chain genes is driven by a powerful actin 15 promoter and the genes are present in multiple copies per cell (*31*, *41*, *42*). It was later demonstrated that myosin or its head fragments without light chain binding domains are expressed at much higher levels than the native protein expressed in the same cell line (*1*, *2*, *43*). We thus hypothesized that the expression levels are limited by the amount of light chains, and overexpression of light chain genes would increase the expression levels of recombinant myosin II and its fragments.

On the basis of this rationale, we have constructed an expression plasmid that carries genes for the S1 heavy chain, essential light chain, and regulatory light chain, each fused with an actin 15 promoter (Figure 1). Introduction of this plasmid into myosin II null cells resulted in higher levels of S1 expression, which was severalfold higher than that obtained with a plasmid carrying the heavy chain gene only (Figure 2). A yield of 5−10 mg of S1/10 g of cells was routinely attained, and this overexpression system was used throughout this study.

Light Scattering Assay. We have previously shown by cosedimentation assays that G680V S1 efficiently binds to actin even in the presence of ATP (*30*). We reexamined this point using a light scattering assay. Addition of wild-type S1 significantly increased light scattering of an actin solution, and subsequent addition of ATP reduced the scattering almost to the initial value (Figure 3A), consistent with previous reports. Addition of G680V S1 also increased the light scattering of an actin solution, but subsequent addition of

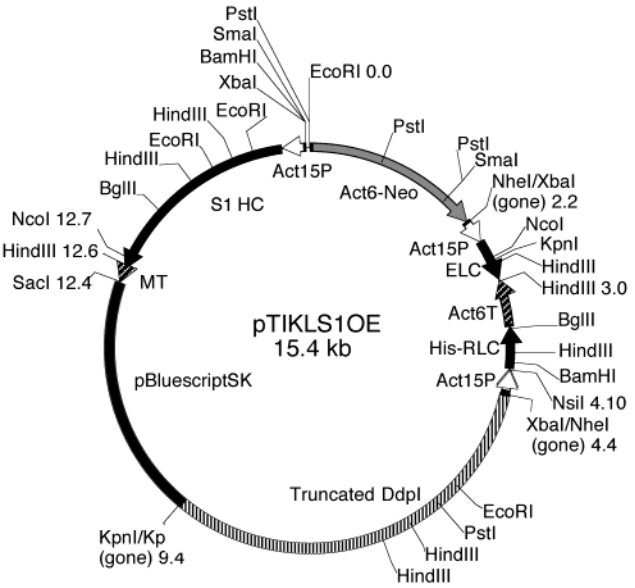

FIGURE 1: pTIKLS1OE, a plasmid for overexpression of S1. All sites of each indicated restriction enzyme are shown, except that there is an extra *Sac*I site somewhere in the light chain gene region.

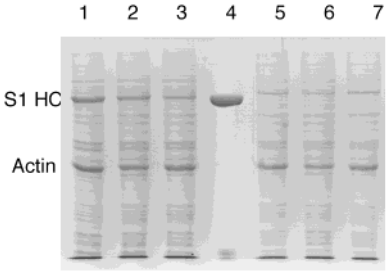

FIGURE 2: Overexpression of wild-type S1. Lanes 1−3 are total lysates of *mhcA* null cells carrying pTIKLS1OE. Lanes 5−7 are those of cells carrying pTIKLS1, similar to pTIKLS1OE but without the two light chain genes. Lysates from the same weight of cells were loaded on each lane of 7.5% acrylamide gel and were stained with Coomassie Blue. Lane 4 is purified S1.

ATP decreased the value by only 40% (Figure 3B). This lessened response to ATP is consistent with our earlier cosedimentation data and indicates that the majority of the G680V mutant remains bound with actin in the presence of ATP.

Following the rapid, partial decrease, the light scattering of acto−680V S1 in the presence of ATP slowly and steadily increased thereafter. Fluorescence microscopic observation of actin filaments labeled with rhodamine phalloidin indicated that samples processed in a similar way are extensively bundled (not shown). Thus, we speculate that at least a part of the steady increase of light scattering of acto−680V S1 in the presence of ATP reflects an actin bundling reaction. This bundling is not specific to the G680V mutation, because acto−wild-type S1 under rigor conditions bundles in a similar manner (not shown).

Pyrene−Actin Quenching Assay. The nature of the acto−G680V S1 complex in the presence of ATP was investigated using another assay, which measures fluorescence quenching of a pyrene moiety bound to Cys 374 of actin. It is well established that the fluorescence of this pyrene is strongly quenched when the motor domain of skeletal muscle or *Dictyostelium* myosin II is bound to actin in the absence of ATP (*35*, *38*, *44*). Wild-type S1 added to the same molar

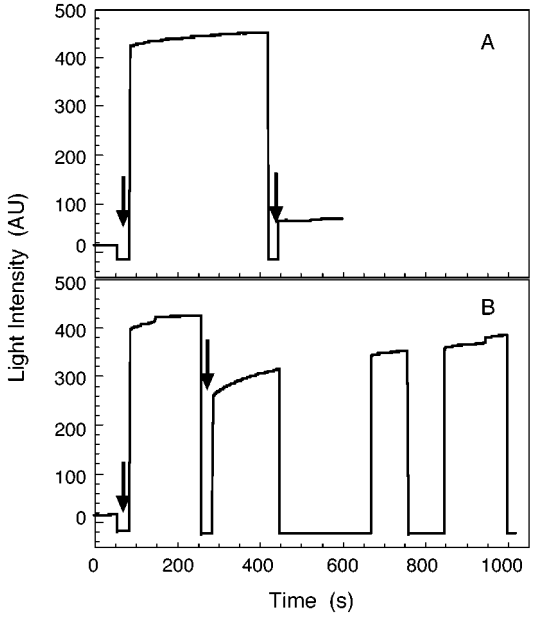

FIGURE 3: Light scattering of acto−S1 solutions: (A) wild-type S1; (B) G680V S1. S1 was added to a final concentration of 2 μM to a 2 μM solution of actin filaments at the first arrow, to which 1 mM ATP was subsequently added at the second arrow. The shutter was closed when the light intensity takes negative values.

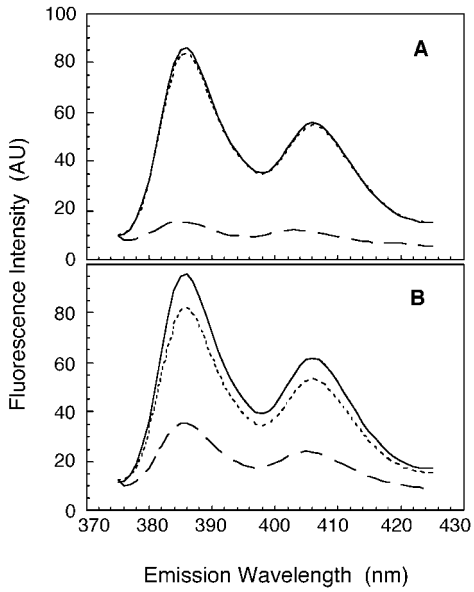

FIGURE 4: Fluorescence spectrum of actin-bound pyrene in the presence of S1. The solid lines are emission spectra of 1 μM pyrene-labeled actin solution, the broken lines represent those after addition of equimolar concentrations of wild-type (A) or G680V (B) S1, and the dotted lines are after subsequent addition of 1 mM ATP.

concentration as the pyrene−actin subunits quenched the fluorescence of pyrene to ~20% of the value of the pyrene−actin solution, and subsequent addition of ATP restored the fluorescence intensity almost to the original value (Figure 4A). An equimolar concentration of G680V S1 also quenched the fluorescence intensity of the pyrene−actin solution, although the extent of quenching was somewhat weaker than that of wild-type S1 at about 40% (38% in the data shown in Figure 4B and 44% in the data shown in Table 1) of the original value. Addition of a 60% molar excess of G680V S1 did not cause further quenching (not shown). Surprisingly, addition of ATP restored the fluorescence intensity to the

Table 1: Quenching of Pyrene Fluorescence and Light Scattering of Pyrene−Acto−S1 in the Presence of Nucleotides[a]

	no nucleotide		+ATP		+ADP	
	pyrene fluorescence (%)	light scatter (%)	pyrene fluorescence (%)	light scatter (%)	pyrene fluorescence (%)	light scatter (%)
WT	19	923	94	117	24	990
G680V	44	906	96	574	39	896

[a] Each data point is a relative value compared with the light intensity of the pyrene−actin solution without S1. Concentrations of ATP and ADP were 0.5 mM and 0.1 mM, respectively, and measurements were made 3 min after the addition of the nucleotide.

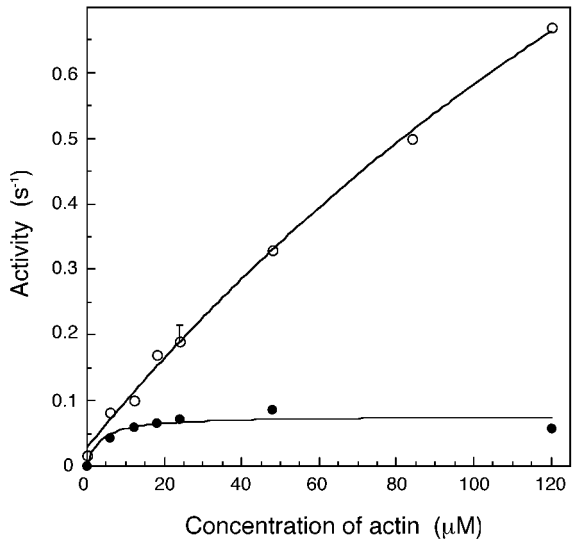

FIGURE 5: Steady-state ATPase activities. MgATPase activities of wild-type and G680V S1 were measured in the presence of varying concentrations of actin filaments. Open circles: wild-type S1. Closed circles: G680V S1. Each data point at 0 and 24 μM actin was measured three times and is shown as the average ± SD (some of the error bars are hidden behind the symbols).

86% level of the original value, even though cosedimentation and light scattering assays indicated that the majority of G680V S1 is bound to actin in the presence of ATP.

Wild-type S1 carrying ADP quenches the pyrene fluorescence as efficiently as the rigor complex in the absence of nucleotides (Table 1). This was also true with G680V S1, although the extent of quenching was again somewhat weaker than that of wild-type S1 (Table 1).

Steady-State ATPase Activities. The MgATPase activities of wild-type and G680V S1 were measured over a range of actin concentrations (Figure 5). In the absence of actin, G680V S1 hydrolyzed ATP at a very low rate of 0.00070 ± 0.00022 s^{-1} ($N = 3$), which was much lower than that of wild type (0.016 ± 0.0007 s^{-1}). Low concentrations of actin filaments efficiently enhanced the MgATPase activity of G680V S1, to 0.072 ± 0.0035 s^{-1} in the presence of 24 μM actin filaments. Fitting of the data with the Michaelis−Menten equation yielded K_{app} of 3.4 μM. The activities of wild-type S1 did not saturate even with the highest concentration of actin filaments tested, and we were unable to determine the value of its K_{app}. It is, however, apparent that the K_{app} value of wild-type S1 is at least 20-fold higher than that of G680V S1. In contrast, V_{max} of wild-type S1 was >0.7 s^{-1}, at least 10-fold higher than that of G680V S1 (0.076 s^{-1}).

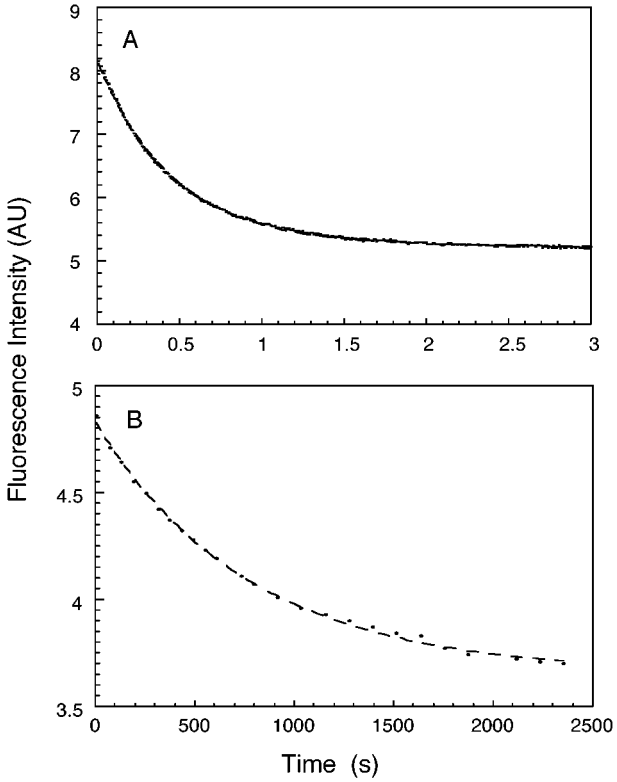

FIGURE 6: Time course of mant-ADP release from S1. Decrease in mant fluorescence was followed after rapid mixing of S1 carrying mant-ADP and excess ATP. One syringe of the stopped-flow apparatus contained 4 μM S1 and 4 μM mant-ADP in 25 mM KCl, 4 mM $MgCl_2$, 1 mM DTT, and 10 mM HEPES, pH 7.4, and the second syringe contained 200 μM ATP in the same buffer. (A) Wild-type S1. (B) G680V S1. G680V S1 was incubated with mant-ADP on ice overnight before the experiment, and to avoid bleaching of the dye due to the very slow process, the shutter for the excitation light and data acquisition were controlled manually. Dashed lines represent fitting with single exponentials.

An ATP regeneration system was not included in these measurements, and therefore possible effects of ADP buildup in the reaction mixtures were examined. At the end of each reaction there was approximately 20 μM ADP buildup, and the average concentration of ADP during the reaction was around 10 μM. Thus, ATPase activities of G680V S1 in the presence of 24 μM actin and 1 mM ATP with or without 20 μM ADP were compared. This exogenously added 20 μM ADP reduced the activity by ~4%, indicating that the average concentration of 10 μM ADP buildup in the reaction mixtures had only negligible effects on the activities. This conclusion was further supported by the fact that there was no apparent reduction in activities among three time segments bordered by four time points taken for each measurement (not shown).

Rates of ADP and Phosphate Release. To determine which step in the ATPase cycle is rate limiting and which chemical state in the cycle is overoccupied, rates of ADP release and phosphate release were compared between wild-type and G680V S1.

The rate constants of ADP release from S1were estimated by measuring the rate constants of mant-ADP release following addition of excess ATP. Wild-type S1 released mant-ADP at a rate of 2.15 s^{-1}, whereas G680V S1 released at an extremely slow rate of 0.0013 s^{-1} (Figure 6). Considering the possible difference in affinities for ADP and mant-

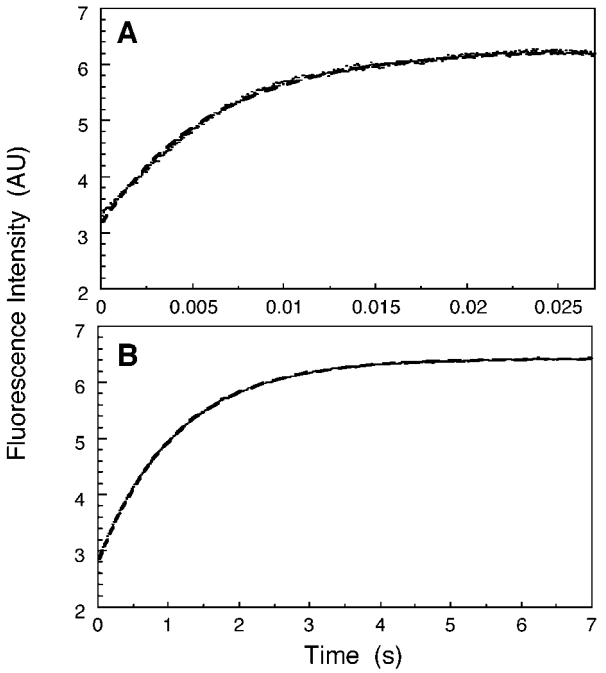

FIGURE 7: Time course of ATP-induced dissociation of the acto−S1 complex carrying ADP. The increase in pyrene fluorescence was followed after rapidly mixing the complex of pyrene−actin filaments and S1 carrying ADP with excess ATP. One syringe of the stopped-flow apparatus contained 4 μM S1, 4 μM pyrene−actin filaments, 4.8 μM phalloidin, 50 μM ADP in 100 mM KCl, 4 mM $MgCl_2$, 1 mM DTT, and 10 mM HEPES, pH 7.4, and the second syringe contained 5 μM ATP in the same buffer. (A) Wild-type S1. (B) G680V S1. Dashed lines represent fitting with single exponentials.

ADP, release of ADP may well be rate limiting in the steady-state ATPase cycle of G680V S1 (0.0007 s^{-1}).

The rate constants of ADP release from acto−S1 were indirectly estimated by observing increase in pyrene fluorescence when pyrene−acto−S1 carrying ADP was mixed with excess ATP (Figure 7). G680V S1 released ADP at a rate of 0.90 s^{-1}, which was more than 2 orders of magnitude slower than that of wild type (140 s^{-1}). Nonetheless, the rate of ADP release is much faster than the rate of steady-state ATP hydrolysis by acto−G680V S1 (0.072 s^{-1}), suggesting that ADP release is not rate limiting in the presence of actin.

Next, rates of phosphate release were compared when nucleotide-free S1 was mixed with a solution containing 4 μM ATP and 48 μM actin filaments (Figure 8). As a precaution to rule out the possible effects of ADP contamination, the S1 solutions were treated with 0.04 unit/mL apyrase for 20 min at room temperature, and the actin solutions were dialyzed against a nucleotide-free buffer and further treated with Dowex anion-exchange resin immediately before use. Traces of phosphate release by both wild type and the mutant S1 were reasonably well fit by single exponentials, and the rate constants were 0.44 s^{-1} for the wild type and 0.050 s^{-1} for G680V S1.

To rule out the possibility that this apparent slow rate of phosphate release of G680V S1 is due to its slower rate of binding to very low concentrations of ATP, the rates of ATP binding were estimated indirectly by measuring the rates of ATP-induced dissociation of S1 from pyrene−actin filaments. When 0.25 μM pyrene−acto−S1 was mixed with 4 μM ATP, G680V S1 dissociated at a rate of 0.25 s^{-1}, whereas

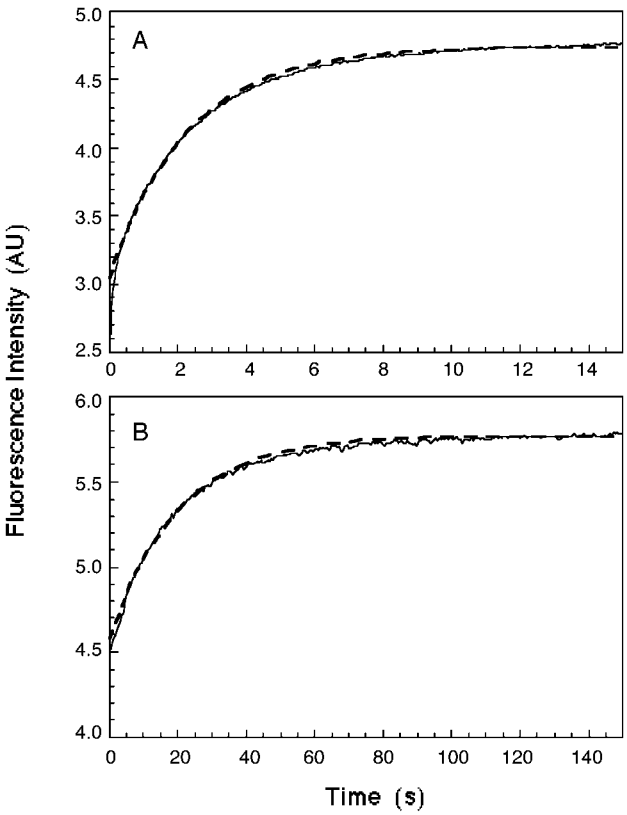

FIGURE 8: Time course of phosphate release. Phosphate release was followed by monitoring the fluorescence change of MDCC−PBP after rapid mixing of S1 with ATP. One syringe of the stopped-flow apparatus contained 4 μM S1, 10 μM MDCC−PBP, 100 μM 7-methylguanosine, 0.04 unit/mL apyrase, 0.02 unit/mL purine nucleoside phosphorylase in 25 mM KCl, 4 mM $MgCl_2$, 1 mM DTT, and 10 mM HEPES, pH 7.4, and the second syringe contained 4 μM ATP, 48 μM actin filaments, 100 μM 7-methylguanosine, and 0.02 unit/mL purine nucleoside phosphorylase in the same buffer. (A) Wild-type S1. (B) G680V S1. Dashed lines represent fitting with single exponentials.

the rate of wild-type S1 was 0.72 s^{-1} (Figure 9). Thus, the rate of ATP binding may be slowed by the G680V mutation, but it is still much faster than the rate of phosphate release under the same experimental conditions.

To determine if ATP hydrolysis itself is rate limiting in the ATPase cycle of G680V S1, [α-^{32}P]ATP was added to a solution of G680V S1, and the relative amounts of ATP and ADP were determined after quenching by manual addition of perchloric acid. However, our preliminary experiments failed to obtain quantitative generation of ADP within 10−100 s, probably because a large fraction of our G680V S1 molecules have bound ADP, which is only very slowly released even when there is excess ATP (Figure 6B). Thus, to accelerate the release of carryover ADP, experiments were performed in the presence of actin filaments. When the reaction was terminated at 6 s after the addition of 100 μM ATP to acto−G680V S1 solutions, 1.27 mol of ADP was generated per mole of G680V S1 ($N = 3$); 1.16 mol of ADP was generated per mole of G680V S1 within 6 s, when the KCl concentration in the reaction mixture was raised from 25 to 100 mM to slow the acto−G680V S1 reassociation. Because 6 s is much shorter than the ATP turnover rate of acto−G680V S1 (13.9 s), these results demonstrate that ATP hydrolysis is not rate limiting in the steady-state ATP hydrolysis cycle of acto−G680V S1.

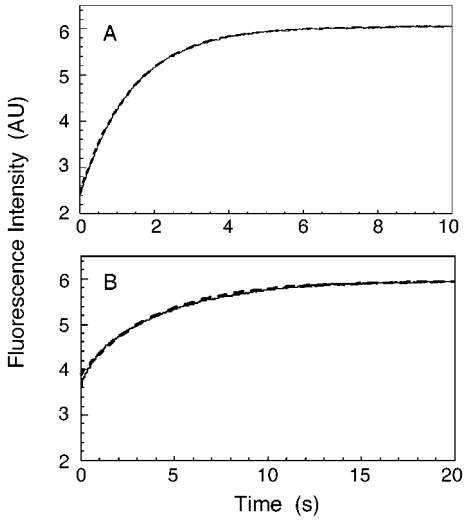

FIGURE 9: Time course of ATP-induced acto−S1 dissociation. One syringe of the stopped-flow apparatus contained 0.25 μM S1, 0.25 μM pyrene−actin filaments, 0.3 μM phalloidin in 25 mM KCl, 4 mM $MgCl_2$, 1 mM DTT, and 10 mM HEPES, pH 7.4, and the second syringe contained 4 μM ATP in the same buffer. (A) Wild-type S1. (B) G680V S1. Dashed lines represent fitting with single exponentials.

Kinetics of Actin Binding of S1 Carrying ADP and P_i. Finally, changes in light scattering and pyrene fluorescence were compared between wild-type and G680V S1 when acto−S1 complexes went through one round of ATP hydrolysis. This was accomplished by adding ATP to complexes between S1 and pyrene-labeled actin filaments and monitoring subsequent changes in pyrene fluorescence and light scattering using a stopped-flow apparatus. To achieve rapid initial ATP binding while simultaneously preventing subsequent ATP binding, 50 μM ATP was added to the rigor complexes, along with 25 units/mL hexokinase and 2 mM glucose, which degraded the unbound ATP. The initial ATP concentration of 50 μM was chosen because a preliminary experiment to measure rates of ATP-induced acto−S1 dissociation had shown ATP binding to wild-type or G680V S1 is much faster than the acto−S1 rebinding in the presence of this concentration of ATP (data not shown). That ATP was efficiently removed before the second cycle began was demonstrated by the observation that adding a 2-fold higher concentration of hexokinase did not affect the result (not shown).

Light scattering of acto−wild-type S1 rapidly decreased upon being mixed with ATP, representing ATP-induced dissociation of the rigor acto−S1 complex (Figure 10A). This was followed by slow recovery close to the original value, as the proteins reassociate following hydrolysis. Fitting of this recovery phase with a single exponential yielded a rate constant of 0.31 s^{-1}. Pyrene fluorescence showed a change that is almost a mirror image of that of light scattering. It increased rapidly and then slowly decreased, approaching the original value. Fitting of the slow decrease phase yielded a rate constant of 0.27 s^{-1}, demonstrating that the increase of light scattering and the decrease of pyrene fluorescence almost coincide with each other.

G680V S1 behaved differently from wild-type S1 in two ways (Figure 10B). First, the rapid phase of both light scattering and pyrene fluorescence is faster than with wild type. Second, the recovery (slower) phases of the light

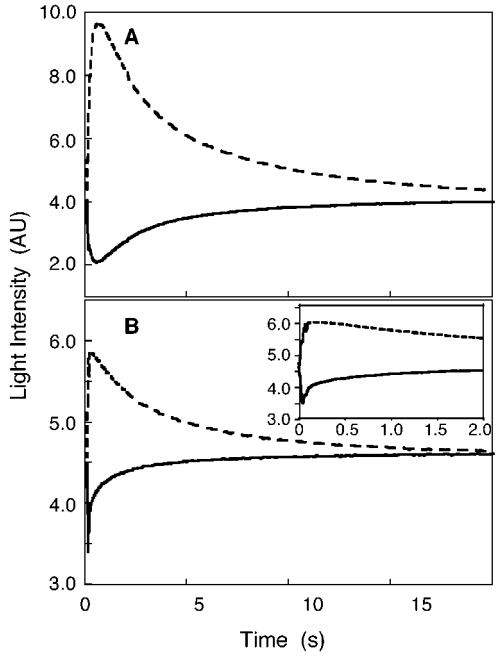

FIGURE 10: Time course of pyrene fluorescence and light scattering changes during one cycle of ATP hydrolysis. One syringe contained 4 μM S1, 48 μM pyrene−actin filaments, 60 μM phalloidin and 50 units/mL hexokinase in 10 mM NaCl, 1 mM $MgCl_2$, and 5 mM imidazole, pH 7.4, and the second syringe contained 100 μM ATP and 4 mM glucose in the same buffer. Broken lines: pyrene fluorescence. Solid lines: light scattering. (A) Wild-type S1. (B) G680V S1.

scattering and pyrene fluorescence have different rate constants. The slow phase of pyrene fluorescence has a rate constant (0.29 s^{-1}) similar to that of the wild type. However, the recovery of light scattering had a rate constant of 2.9 s^{-1}, ~10-fold faster than wild type, suggesting that the proteins reassociate faster than with wild type. This suggests that G680V S1 carrying ADP and P_i binds to actin and then spends ~2.5 s bound with actin in a conformation that scatters light but does not quench the pyrene fluorescence. This is consistent with the steady-state data in Figures 3 and 4, and the biochemical implications are discussed below.

DISCUSSION

We have previously shown that *Dictyostelium* myosin II carrying the G680V mutation binds strongly to actin even in the presence of ATP (*27*) and, on the basis of biochemical phenotypes of suppressor mutations, suggested that G680V mutant motors suffer from accumulation in the prestroke A·M·ADP·P_i state (Scheme 1) (*28*, *29*). In this study we have further characterized the interaction between G680V S1 and actin filaments by examining light scattering, fluorescence quenching of pyrene attached to actin, and direct measurements of the ADP and P_i release rates.

Steady-state light scattering analysis yielded data that are fully consistent with the cosedimentation data. However, the fluorescence changes of a pyrene molecule bound to actin suggest that this bound mutant is not in a typical rigor or ADP-bound state. Specifically, the pyrene fluorescence of the bound complex is similar to that of free actin whereas bound wild-type motors in rigor or ADP-bound states typically quench the fluorescence by severalfold. This result, as well as the kinetic data on ATP hydrolysis, ADP release,

and phosphate release discussed below, supports our previous contention that A·M, A·M·ATP, or A·M·ADP are not the main intermediates in G680V mutant motors during steady-state ATPase activity.

Direct measurement of rates of phosphate release demonstrates that G680V S1 is slower than wild type at the phosphate release step or step(s) preceding it. G680V S1's rate constant of phosphate release was 0.05 s^{-1} in the presence of 24 μM actin filaments. This reduced rate is sufficiently slow to account for the mutant's reduced rate of steady-state ATP hydrolysis (0.072 s^{-1}), which was assayed under the same conditions except for the concentration of ATP. The slower rate of phosphate release than the steady-state hydrolysis is at least in part due to the lower concentration of ATP used in the phosphate release assay. In addition, we speculate that this discrepancy is also partly due to the fact that actin filaments and G680V S1 form bundles even in the presence of ATP, which would increase the effective concentration of actin filaments in the steady-state measurements but not in the single turnover phosphate release assay.

These results imply that a step between ATP binding and phosphate release is rate limiting in the ATPase cycle of acto−G680V S1. G680V S1 binds ATP slower than wild type in the presence of 2 μM ATP, but the rate is still much faster than the rate of phosphate release and thus cannot be rate limiting. We were unable to determine quantitatively the rate constant of ATP hydrolysis by G680V S1, because its tryptophan fluorescence does not change upon addition of ATP (Uyeda, Malnasi-Csizmadia, and Bagshaw, unpublished data). However, we were able to show that 1 mol of G680V S1 in the presence of actin filaments generates 1.27 mol of ADP within 6 s after the addition of ATP. Furthermore, we have previously shown that G680V S1 does not cosediment with actin filaments efficiently in the presence of ATPγS, suggesting that hydrolysis of ATP is required to allow G680V S1 to bind actin (*27*). These two pieces of evidence strongly argue against the possibility that ATP hydrolysis is rate limiting and the most populous state in the presence of ATP is the A·M·ATP state. Finally, the single turnover light scattering assay (Figure 10) demonstrated that G680V S1 binds actin filaments more rapidly than the wild type in the presence of ATP, indicating that the overall rate of ATP binding, hydrolysis, and actin binding by G680V S1 is faster than by wild type.

Batra et al. (*37*) carried out kinetic analyses on a mutant *Dictyostelium* myosin head fragment that changed the same Gly 680 to Ala. Our previous studies have suggested that this mutant is similar to, but milder than, the G680V mutant (*30*). Most notably, they reported that the G680A mutant is 20−30-fold slower in nucleotide binding and has a 10-fold higher affinity for ADP, due to a 200-fold reduction in the dissociation rate. This is consistent with our previous finding that the apparent affinity of G680V myosin for ADP is higher in a steady-state cosedimentation assay (*30*). In this study, we have directly shown that dissociation of mant-ADP from G680V S1 is extremely slow (0.0013 s^{-1}), which is several-fold slower than that of G680A (0.01 s^{-1}) (*37*). Dissociation of ADP from acto−G680V S1 is also slow (0.90 s^{-1}) (Figure 7) and, again, slower than the rate reported for G680A by Batra et al. (3.1 s^{-1}) (*37*). Nonetheless, the rate of ADP release from acto−G680V S1 is much faster than the rate of the steady-state ATPase cycle (0.076 s^{-1}) or the rate of phosphate release (0.050 s^{-1}). Furthermore, even though acto−G680V S1 efficiently quenches the pyrene fluorescence in the presence of ADP, the quenching is only partial in the presence of ATP despite the high light scattering. These results indicate that ADP release is not rate limiting in the steady-state ATPase hydrolysis cycle of acto−G680V S and the A·M·ADP state is not the overoccupied state in the presence of ATP. On the basis of these results, we conclude that phosphate release is rate limiting in the steady-state ATP hydrolysis cycle of acto−G680V S1. We also conclude that acto−S1 carrying ADP and P_i is the main steady-state intermediate and that this state does not quench pyrene fluorescence.

Scheme 2

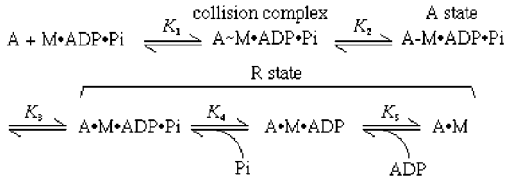

This conclusion is particularly relevant to the "3G" model proposed by Geeves et al. (*45*, *46*) to describe the sequence of structural events leading to the formation of the A·M complex in the mechanical cycle. This model hypothesizes that actin and the myosin motor domain first form a collision complex and then form a stereospecific "A state" complex with an intermediate affinity. This is followed by an isomerization, which is hypothesized to correspond to the power stroke, to the "R state" or the rigor state, with the strongest affinity. On the basis of pressure-jump experiments, it is further hypothesized that the A state complex scatters light but does not quench the fluorescence of pyrene actin (*47*).

The three criteria used by Geeves and his colleagues to characterize the A state, positive light scattering, negative fluorescence quenching, and intermediate affinity, perfectly match the properties of the overoccupied state of acto−G680V S1 in the presence of ATP. This coincidence suggests that the overoccupied state of the acto−G680V motor domain in the presence of ATP is a genuine intermediate state of the acto−myosin ATPase cycle. That the overoccupied state of the acto−G680V ATPase cycle is not an artifactual or off-cycle conformation due to the mutation is further supported by the fact that the G680V mutation and a number of other mutations can be restored to function by secondary changes elsewhere in the molecule (suppression). This mutual suppression is consistent with the idea that the G680V and other mutations each primarily affect stability of a state or equilibrium between states or alter the kinetic barrier between two states in one way or the other. This model predicts that a proper combination of two mutations partially restores an appropriate equilibrium or a kinetic rate and, consequently, the function.

In the 3G model, the A and R states are not in one-to-one correspondence with specific chemical states. However, if the force-generating conformational change of cross-bridges occurs prior to the phosphate release step (*13*), it would be reasonable to place the A to R transition before the phosphate release step in the normal acto−S1 ATPase cycle (Scheme 2).

The similarity of the overoccupied state in the steady-state acto−G680V S1 ATPase cycle and the A state suggests that

the overoccupied state in the acto−G680V S1 ATPase cycle would correspond to the A−M·ADP·P_i state (A state) in Scheme 2. In this model, there are two possible mechanisms on how the G680V mutation results in accumulation of the A−M·ADP·P_i state. One is that k_3, the rate constant of transition from the A−M·ADP·P_i state to the A·M·ADP state, is reduced, without significantly affecting other rates or equilibrium between states. This model assumes that K_2 is small, such that the reduction in k_3 results in accumulation of the A−M·ADP·P_i state alone, rather than together with other states preceding it. This model is consistent with the idea that G680 is a swivel point for a conformational change that leads to the power stroke, and changing this Gly residue to Val simply slows down the rate of this conformational change (*48*). The other possibility is that the A−M·ADP·P_i state is hyperstabilized, so that the rate to form the A−M·ADP·P_i state is accelerated (larger k_2 or k_1 and smaller K_2 or K_1), while the rate exiting from this state is decreased (smaller k_3 and larger K_3). In this latter model, perhaps the bulky side chain of Val creates a structural stress to favor the A−M·ADP·P_i conformation.

Our data are more consistent with this latter model. First, the fluorescence intensities of pyrene−actin bound with G680V S1 in the absence of nucleotides or in the presence of ADP are stronger than that bound with wild-type S1 under corresponding conditions. This result can be interpreted to mean that a fraction of the acto−G680V S1 cross-bridges without nucleotides or with bound ADP take the "preferred" conformation, which does not quench the fluorescence as efficiently as the typical rigor. Second, if the primary defect of G680V mutant S1 is the retarded transition from one state to another due to a physical steric hindrance by the bulky side chain of Val, it is difficult to reconcile how that steric hindrance can be alleviated by point mutations that are some distances away from G680. Indeed, the majority of the suppressor mutations result in *larger* residues; only one suppressor (N483S) is close to G680 in myosin structures, and it is the only one that could potentially "make room" for a larger residue at position 680 (*27*). Finally, G680F mutant myosin behaves more like wild type both in vivo and in vitro than G680V (T. Uyeda, K. Ito, and B. Patterson, unpublished data), despite the larger side chain volume of Phe compared to Val. These data suggest that there is an optimum volume of the side chain at this position that causes this series of intriguing biochemical phenotypes, and the propensity to act as a flexible joint is not critically relevant. If this hyperstabilized conformation has a high affinity for ADP, that would explain why the G680V mutant exhibits a higher affinity for ADP in a steady-state assay (*27*) and also why dissociation of mant-ADP is extremely slow in a transient kinetic assay.

As discussed above, there are two distinct kinetic mechanisms that are able to drive formation of the A−M·ADP·P_i state in the forward direction. Smaller K_1 would imply that the affinity in the weakly bound state is increased, whereas smaller K_2 would imply that a structural change to establish stereospecific contacts between actin and S1 is accelerated once the two molecules form a collision complex. These two are very different mechanisms, but at present we do not have evidence to favor one or the other, and this question awaits further studies. Also, detailed structural analyses of this complex at the electron microscopic and crystallographic levels are underway to investigate whether there is a distinct prestroke cross-bridge conformation and, if it exists, what it looks like.

ACKNOWLEDGMENT

We thank Dr. Kazuo Sutoh for providing us with the ELC and RLC genes fused to the actin promoter and terminator, Dr. Dietmar Manstein for kind assistance in the initial phase of the stopped-flow measurements, Drs. Xue-ying Liu and Chikashi Nakamura for help in the initial phase of ATP hydrolysis assay, and Drs. Eisaku Katayama and Yuichi Hiratsuka for advice and discussions. We also thank Chuai Jing Fan for excellent technical assistance and Jackie Hunter (NIMR, London) for preparing the P_i sensor.

REFERENCES

1. Anson, M., Geeves, M. A., Kurzawa, S. E., and Manstein, D. J. (1996) *EMBO J. 15*, 6069−6074.
2. Uyeda, T. Q. P., Abramson, P. D., and Spudich, J. A. (1996) *Proc. Natl. Acad. Sci. U.S.A. 93*, 4459−4464.
3. Warshaw, D. M., Guilford, W. H., Freyzon, Y., Krementsova, E., Palmiter, K. A., Tyska, M. J., Baker, J. E., and Trybus, K. M. (2000) *J. Biol. Chem. 275*, 37167−37172.
4. Ruff, C., Furch, M., Brenner, B., Manstein, D. J., and Meyhofer, E. (2001) *Nat. Struct. Biol.*, 226−229.
5. Tokunaga, M., Sutoh, K., and Wakabayashi, T. (1991) *Adv. Biophys. 27*, 157−167.
6. Wakabayashi, K., Tokunaga, M., Kohno, I., Sugimoto, Y., Hamanaka, T., Takezawa, Y., Wakabayashi, T., and Amemiya, Y. (1992) *Science 258*, 443−447.
7. Fisher, A. J., Smith, C. A., Thoden, J. B., Smith, R., Sutoh, K., Holden, H. M., and Rayment, I. (1995) *Biochemistry 34*, 8960−8972.
8. Dominguez, R., Freyzon, Y., Trybus, K. M., and Cohen, C. (1998) *Cell 94*, 559−571.
9. Suzuki, Y., Yasunaga, T., Ohkura, R., Wakabayashi, T., and Sutoh, K. (1998) *Nature 396*, 380−383.
10. Huxley, H. E. (1963) *J. Mol. Biol. 7*, 281−308.
11. White, H. D., and Taylor, E. W. (1976) *Biochemistry 15*, 5818−5826.
12. Cooke, R., and Pate, E. (1985) *Biophys. J. 48*, 789−798.
13. Dantzig, J. A., Goldman, Y. E., Millar, N. C., Lacktis, J., and Homsher, E. (1992) *J. Physiol.* 247−278.
14. Lymn, R. W., and Taylor, E. W. (1971) *Biochemistry 10*, 4617−4624.
15. He, Z.-H., Chillingworth, R. K., Brune, M., Corrie, J. E. T., Webb, M. R., and Ferenczi, M. A. (1999) *J. Physiol. 517*, 839−854.
16. Funatsu, T., Kono, E., and Tsukita, S. (1993) *J. Cell Biol. 121*, 1053−1064.
17. Hirose, K., Lenart, T. D., Murray, J. M., Franzini-Armstrong, C., and Goldman, Y. E. (1993) *Biophys. J. 65*, 397−408.
18. Holmes, K. C. (1997) *Curr. Biol. 7*, 112−118.
19. Huxley, H. E., and Kress, M. (1985) *J. Muscle Res. Cell Motil. 6*, 153−161.
20. Berger, C. L., and Thomas, D. D. (1994) *Biophys. J. 67*, 250−261.
21. Thomas, D. D., Ramachandran, S., Roopnarine, O., Hayden, D. W., and Ostap, E. M. (1995) *Biophys. J. 68*, 135s−141s.
22. Yanagida, T., Kitamura, K., Tanaka, H., Hikkoshi-Iwane, A., and Esaki, S. (2000) *Curr. Opin. Cell Biol. 12*, 20−25.
23. Kitamura, K., Tokunaga, M., Iwane, A. H., and Yanagida, T. (1999) *Nature 397*, 129−134.
24. Tanaka, H., Homma, K., Iwane, A. H., Katayama, E., Ikebe, R., Saito, J., Yanagida, T., and Ikebe, M. (2002) *Nature 415*, 192−195.
25. Inoue, A., Saito, S., Ikebe, R., and Ikebe, M. (2002) *Nat. Cell Biol. 4*, 302−306.
26. Post, P. L., Tyska, M. J., O'Connell, C. B., Johung, K., Hayward, A., and Mooseker, M. S. (2002) *J. Biol. Chem. 277*, 11679−11683.
27. Patterson, B., Ruppel, K. M., Wu, Y., and Spudich, J. A. (1997) *J. Biol. Chem. 272*, 27612−27617.
28. Patterson, B. (1998) *Genetics 149*, 1799−1807.

29. Wu, Y., Nejad, M., and Patterson, B. (1999) *Genetics 153*, 107−116.
30. Liu, X., Ito, K., Lee, R. J., and Uyeda, T. Q. P. (2000) *Biochem. Biophys. Res. Commun. 271*, 75−81.
31. Ruppel, K. M., Uyeda, T. Q. P., and Spudich, J. A. (1994) *J. Biol. Chem. 269*, 18773−18780.
32. Egelhoff, T. T., Titus, M. A., Manstein, D. J., Ruppel, K. M., and Spudich, J. A. (1991) *Methods Enzymol. 196*, 319−334.
33. Yumura, S., and Uyeda, T. Q. P. (1997) *Mol. Biol. Cell 8*, 2089−2099.
34. Spudich, J. A., and Watt, S. (1971) *J. Biol. Chem. 246*, 4866−4871.
35. Kouyama, T., and Mihashi, K. (1981) *Eur. J. Biochem. 114*, 33−38.
36. Gordon, D. J., Yang, Y. Z., and Korn, E. D. (1976) *J. Biol. Chem. 251*, 7474−7479.
37. Batra, R., Geeves, M. A., and Manstein, D. J. (1999) *Biochemistry 38*, 6126−6134.
38. Kuhlman, P. A., and Bagshaw, C. R. (1998) *J. Muscle Res. Cell Motil. 19*, 491−504.
39. Brune, M., Hunter, J. L., Corrie, J. E., and Webb, M. R. (1994) *Biochemistry 33*, 8262−8271.
40. Kodama, T., Fukui, K., and Kometani, K. (1986) *J. Biochem. 99*, 1465−1472.
41. Manstein, D. J., Ruppel, K. M., and Spudich, J. A. (1989) *Science 246*, 656−658.
42. Ruppel, K. M., Egelhoff, T. T., and Spudich, J. A. (1990) *Ann. N.Y. Acad. Sci. 582*, 147−155.
43. Itakura, S., Yamakawa, H., Toyoshima, Y. Y., Ishijima, A., Kojima, T., Harada, Y., Yanagida, T., Wakabayashi, T., and Sutoh, K. (1993) *Biochem. Biophys. Res. Commun. 196*, 1504−1510.
44. Ritchie, M. D., Geeves, M. A., Woodward, S. K., and Manstein, D. J. (1993) *Proc. Natl. Acad. Sci. U.S.A. 90*, 8619−8623.
45. Geeves, M. A., Goody, R. S., and Gutfreund, H. (1984) *J. Muscle Res. Cell Motil. 5*, 351−361.
46. Geeves, M. A. (1991) *Biochem. J. 274*, 1−14.
47. Coates, J. H., Criddle, A. H., and Geeves, M. A. (1985) *Biochem. J. 232*, 351−356.
48. Kinose, F., Wang, S. X., Kidambi, U. S., Moncman, C. L., and Winkelmann, D. A. (1996) *J. Cell Biol. 134*, 895−909.

BI026177I